Neoplasia • Vol. 6, No. 3, May/June 2004, pp. 248–257 248

www.neoplasia.com

Inhibition of Tumor Growth and Angiogenesis by Soluble EphB4[1]

Georg Martiny-Baron[*,2,3], *Thomas Korff*[*,2], *Florence Schaffner*[*,2], *Norbert Esser**, *Stefan Eggstein*[†], *Dieter Marmé** *and Hellmut G. Augustin**

Departments of *Vascular Biology and Angiogenesis Research, Tumor Biology Center and [†]Surgery, University of Freiburg, Freiburg D-79106, Germany

Abstract

EphB receptors and their ephrinB ligands play a key role in the formation of a regular vascular system. Recent studies have also shown the involvement of Eph/ephrin interactions in malignant tumor progression and angiogenesis. We have generated soluble monomeric EphB4 (sEphB4)–expressing A375 melanoma cells to study the effect of dominant negatively acting sEphB4 on tumor growth and angiogenesis. Soluble EphB4-expressing A375 tumors grown subcutaneously in nude mice show dramatically reduced tumor growth compared to control tumors. The proliferative capacity of sEphB4-expressing cells in monolayer culture is not altered. Yet, sEphB4-expressing A375 cells cannot establish proper cell–cell contacts in three-dimensional spheroids. However, sEphB4 transfectants have reduced proliferation and apoptosis rates when grown in three-dimensional culture *in vitro* or in subcutaneous tumors *in vivo*. Analysis of the vascular phenotype of the tumors revealed a reduction of intratumoral microvessel density in sEphB4-expressing tumors. Corresponding to these mouse experiments, a matched pair analysis of EphB4 and ephrinB2 expression in human colon carcinomas revealed significantly upregulated levels of EphB4 expression compared to adjacent normal tissue. Taken together, the data identify dual effects of sEphB4 on the tumor and the vascular compartment that collectively inhibit tumor growth.

Neoplasia (2004) **6**, 248–257

Keywords: Tumor, angiogenesis, endothelial cells, EphB4, EphrinB2.

Introduction

Eph receptors and their corresponding ephrin ligands comprise the largest family of receptor tyrosine kinases [1,2]. In contrast to classical transmembrane receptor and corresponding secreted ligand signaling systems, both Eph receptors and ephrin ligands are membrane-bound molecules. EphrinA ligands are glycosyl phosphatidyl inositol (GPI)-anchored molecules, whereas ephrinB ligands are transmembrane molecules. EphrinB molecules contain cytoplasmic tyrosine and serine phosphorylation sites and have PDZ domain protein engagement capacity, enabling them to act as signaling molecules themselves [2,3]. EphB/ephrinB receptor ligand interactions therefore mediate bidirectional signaling events on direct cell–cell contact [2,4,5]. These provide positive (attractive) and negative (repulsive) positional guidance cues to EphB/ephrinB–expressing cells and regulate adhesive, migratory, and invasive cellular functions [1,2].

Originally identified as neuronal pathfinding molecules [6], genetic loss-of-function experiments have revealed members of the EphB/ephrinB family as critical mediators of vascular assembly and organization, particularly as they relate to the acquisition of arteriovenous identity [7–9]. Arterial endothelial cells selectively express ephrinB2 and venous endothelial cells preferentially express EphB4 [10,11], and mice with deletions of these molecules exhibit an embryonic lethal phenotype as a consequence of a grossly perturbed vascular architecture [7–9]. Elegant genetic loss-of-function experiments have shown that bidirectional EphB/ephrinB signaling in the vascular system is critically required for proper developmental arteriovenous differentiation [12]. Corresponding functional experiments support an arteriovenous push-and-pull model of vascular morphogenesis and vessel assembly with proangiogenic and arteriolizing functions of ephrinB2 and a repulsive function of EphB4 signaling [13].

Recently, Eph/ephrin interactions have also been shown to transduce positional guidance cues in epithelial cells, most notably during colonic epithelial cell differentiation [14]. The expression of different Eph receptors and ephrin ligands has been reported to occur in a number of carcinomas including colon and lung tumors, suggesting a possible involvement of Eph/ephrin signaling during tumor progression [15–17]. Overexpression of EphA2 induces malignant transformation and confers tumorigenic potential on nontransformed mammary epithelial cells [18]. EphA2 as well as its ligand ephrinA1 were found to be expressed by both endothelial cells and various human tumor cells, thereby establishing a microenvironment

Address all correspondence to: Dr. Hellmut G. Augustin, Department of Vascular Biology and Angiogenesis Research, Tumor Biology Center, Breisacher Str. 117, Freiburg 79106, Germany. E-mail: augustin@angiogenese.de

[1]This work was supported by a grant from the Deutsche Forschungsgemeinschaft (SPP1069 "Angiogenesis": Au83/3-2 and 3-3)

[2]These authors contributed equally to this study.

[3]Present address: Novartis Pharma, Basel Switzerland.

Received 17 November 2003; Revised 22 December 2003; Accepted 22 December 2003.

DOI 10.1593/neo.03457

that stimulates tumor neoangiogenesis by activating EphA2 receptors expressed on angiogenic endothelial cells [17]. Blocking of EphA class receptor activation by competitively acting soluble EphA receptors has been shown to inhibit tumor angiogenesis in two different tumor models [19]. Interestingly, stimulation of EphA2 phosphorylation by an EphA2-specific antibody inhibits the malignant behavior of breast tumor cells, indicating that EphA2 signaling may induce different phenotypes in endothelial and tumor cells [20].

In contrast to the EphA/ephrinA receptor ligand system [21], much less is known about the functions of B class Eph/ephrin molecules during tumorigenesis. Several studies have demonstrated the expression of B class Eph/ephrin molecules in different tumors and suggested a functional relationship between Eph/ephrin expression and tumor progression [16,22–28]. Based on these findings and the established role of bidirectional EphB4/ephrinB2 signaling during angiogenesis, we hypothesized that soluble Eph receptors may interfere with tumor growth and angiogenesis. Consequently, we generated soluble EphB4-expressing A375 melanoma cells and studied their tumorigenic and angiogenic properties. The experiments revealed that soluble EphB4 receptor interferes with tumor growth directly, by affecting tumor cell functions, and indirectly, by inhibiting endothelial cell functions.

Materials and Methods

Cells, Antibodies, Growth Factors, and Reagents

Human umbilical vein endothelial cells (HUVECs) were freshly isolated from human umbilical veins of newborn babies by collagenase digestion. SVEC4-10 (CRL-2181) endothelial cells and A375 melanoma cells (CRL-1619) were from the ATCC (Manassas, VA). Fetal calf serum (FCS) was obtained from Biochrom (Berlin, Germany). Endothelial cell growth medium (ECGM) and endothelial cell growth supplement (HUVEC culture) were purchased from Promocell (Heidelberg, Germany). Recombinant mouse EphB4-Fc, anti– murine EphB4 antibody, and human recombinant vascular endothelial growth factor (VEGF) were obtained from R&D Systems (Wiesbaden, Germany). Rat anti–mouse CD31 antibody MEC 13.3 was purchased from Pharmingen (Hamburg, Germany). Rat anti–mouse CD34 antibody MEC 14.7 was obtained from HyCult (Uden, The Netherlands). The proliferation marker rabbit anti–human phospho-H3 was from Upstate Biotechnology (Biomol, Hamburg, Germany). Soluble mouse monomeric EphB4 (sEphB4) was produced by extracting and reverse-transcribing RNA from RENCA tumors [29] using primers specific for the extracellular domain of EphB4 (1.620-bp fragment of bp 1–1620 corresponding to aa 1–540). The sequence was amplified by reverse transcription polymerase chain reaction (RT-PCR) and verified by sequencing. The fragment was subcloned in frame with 6 × His–Myc tags into KS vector (*Nco*I digest). The extracellular domain of EphB4 with 6 × His–Myc tags was subcloned into pVL1392 vector (Biosciences, Heidelberg, Germany). Sf9 insect cells were infected with Baculogold DNA (pACGP67A; Pharmingen) and pVL1392mEphB4-Myc. The protein produced in the Sf9 supernatant was purified by coupling with agarose beads (Qiagen, Hilden, Germany) overnight at 4°C. Samples were passed through a column, washed, and eluted by adding 100 mM imidazole. Different fractions were analyzed by silver staining, dialyzed against phosphate-buffered saline (PBS), and stored at −20°C.

Transfection and Selection of A375 Melanoma Cells

Soluble monomeric EphB4-transfected A375 melanoma cells were generated by transfecting the cells with the 1.620 bp sEphB4 cDNA subcloned into pCDNA3 vector (Invitrogen, Karlsruhe, Germany) using the mammalian transfection kit (Stratagene, Amsterdam, The Netherlands) according to the manufacturer's instructions. Transfected cells were propagated by cell culture in Dulbecco's modified Eagle's medium (DMEM) selection medium containing 10% FCS and 1 mg/ml G418.

RT-PCR

Total cellular RNA was isolated from A375 by using the RNAeasy kit (Qiagen) according to the manufacturer's instructions. cDNA were synthesized using 1 μg of RNA preheated to 65°C for 10 minutes. The cDNA synthesis was done with RT (Invitrogen), 1 × first strand buffer (Invitrogen), 25 mM dNTP (PeqLab, Erlangen, Germany), 0.1 M DTT (Invitrogen), and random primers (Biolaboratories, Beverly, MA) for 1 hour at 37°C. For each reaction, a control without RT was processed in parallel. For PCR reactions, 1 μl of cDNA was mixed with specific primers (10 pmol each), 2.5 U of Taq DNA polymerase (Invitrogen), 5 μl of 10 × reaction buffer, and 10 nmol of dNTPmix (PeqLab) in a final volume of 50 μl. PCR reactions were carried out in a Perkin-Elmer thermocycler (Perkin-Elmer, Norwalk, CT) as follows: 2 minutes at 94°C, 30 seconds at 94°C, 60 seconds at 60°C or 55°C, followed by 60 seconds at 72°C for 35 cycles. The last cycle was terminated with 7 minutes at 72°C. The following primers were used: EphB1s: CTG AAC ACC ATC CGC ACC TAC C; EphB1as: CCC CGT AGT AGA GTT TGA T; EphB2s: CTG TCC CGC AGC GGC TTC; EphB2as: GGC CCC TTC AGA AGT GGT CC; EpB3s: GAA TCC CAT CCG CAC ATA CCA G; and EphB3as: GCA CCC ACA GGC ACC ATC CAC T.

Northern Blot Analysis

Total cellular RNA was isolated from cultured cells and matched pair biopsies of human colon tumors and adjacent tissue were taken at surgery. RNA was separated in formaldehyde-containing agarose gels, transferred to nylon membranes, and hybridized to ^{32}P-DNA–labeled EphB4 and ephrinB2 probes (950-bp human EphB4 probe from the extracellular domain; 1.002-bp full-length human ephrinB2) as described previously [30].

Western Blot Analysis

Mock and transfected A375 cells were cultured for 48 hours, and conditioned media were collected and incubated

overnight with 1 μg of ephrinB2-Fc precoupled with protein G agarose. Precipitates were washed, denatured, and run on a 10% sodium dodecyl sulfate polyacrylamide gel electrophoresis (SDS-PAGE) gel. Then probes were blotted onto a PVDF membrane (Amersham Pharmacia), blocked with a 3% bovine serum albumin (BSA) solution, and incubated with goat anti–murine EphB4 (R&D Systems). After adding rabbit-anti-goat HRP (DAKO, Glostrup, Denmark), the probes were visualized by chemiluminescence (expected size, 75 kDa).

Proliferation Assay

Wild-type and sEphB4-transfected A375 cells were seeded at a density of 10^3 cells per 75 cm^2 in DMEM containing 10% FCS. The cell number was determined by counting the cells in five randomly selected microscopic fields (× 100 magnification), 6 hours (day 0) and every 24 hours thereafter for 7 days.

Soft Agar Colony Assay

Cells (5×10^3) per well in top agarose (0.5 ml of 0.4% agarose in DMEM/5% FCS) were layered onto bottom agarose (0.5 ml of 0.4% agarose in DMEM, 5% FCS) in 24-well plates. Cells were incubated for 14 days at 37°C, and the colonies were counted.

Cell Cycle Analysis by Fluorescence-Activated Cell Sorter (FACS)

Colonies grown in soft agar for 13 days were picked and dissociated with 0.02% EDTA in PBS to obtain a single-cell suspension. Cells were counted in a Neubauer chamber and fixed in methanol. The cells were pelleted, rehydrated in PBS for 30 minutes, pelleted again, and stained in a solution of 25 μg of propidium iodide and 100 μg of RNase A per milliliter for 30 minutes. Flow cytometric analysis was performed on a Becton Dickinson (Heidelberg, Germany) FACS Calibur, and data from 10,000 cells per sample were analyzed with the CellQuest Cell Cycle Analysis software (Becton Dickinson).

Generation of Three-Dimensional Spheroids

A375 melanoma and HUVEC spheroids of defined cell number were generated as described previously [31]. Cells were suspended in culture medium containing 0.25% (wt/vol) methylcellulose and seeded in nonadherent round-bottom 96-well plates (Greiner, Frickenhausen, Germany). Under these conditions, all suspended cells contribute to the formation of a single spheroid per well of defined size and cell number (A375 melanoma cells: 3000 cells/spheroid; HUVEC: 750 cells/spheroid).

In Vitro Angiogenesis Assay

In vitro angiogenesis in collagen gels was quantitated using endothelial cell spheroids as described previously (www.spherogenex.de) [32]. In brief, spheroids containing 750 cells each were generated overnight after which they were embedded into collagen gels. The gels were incubated at 37°C, 5% CO_2, and 100% humidity. After 24 hours, *in vitro* angiogenesis was digitally quantitated by measuring the length of the sprouts that had grown out of each spheroid (ocular grid at × 100 magnification) using the digital imaging software DP-Soft (Olympus, Hamburg, Germany) analyzing at least 10 spheroids per experimental group and experiment.

Xenograft Experiments

Female athymic nude mice (NMRI *−nu/−nu*) were purchased from Elevage Janvier (Le Genest-St-Isle, France). The mice were housed and maintained under controlled conditions in individually ventilated cages (IVCs) (Ventirack, Biozone, UK) and routinely used at 6 to 8 weeks of age. All experiments were carried out according to the guidelines of the Animal Committee of the Regierungspräsidium Freiburg (Germany). The subcutaneous injection of 1×10^6 cells into the dorsal flanks was performed using a 29-gauge needle syringe. Tumor growth was quantitated by caliper measurements every other day. Tumor volume (mm^3) was calculated by calipering the largest diameter (*a*) and its perpendicular (*b*) according to the formula, $0.5ab^2$. Animals were sacrificed on day 16 and tumors were weighed and processed for morphological analysis.

Histochemical Analysis

Paraffin sections (4 μm) and cryosections (5 μm) were cut for histochemical analyses. Deparaffinized and rehydrated paraffin sections and cryosections were incubated with 3% H_2O_2 to inhibit endogenous peroxidase. After washings in PBS, the sections were incubated for 30 minutes with blocking solution (10% normal rabbit serum) followed by incubation with the corresponding primary antibody (anti–mouse CD34, MEC 14.7; anti–mouse CD31, MEC 13.3) in a humid chamber at room temperature for 2 hours. They were then incubated with secondary antibody (biotinylated rabbit anti–rat immunoglobulin antibody) and exposed to streptavidin peroxidase, developed with diaminobenzidine as substrate, and weakly counterstained with Meyer's Hemalaun. Microvessel density was determined by counting the number of $CD34^+$ blood vessels within five randomly selected areas (high-power field, × 200) of two sections of each tumor.

For double immunofluorescence analyses, 4% paraformaldehyde (PFA) postfixed cryosections were probed with primary antibodies against CD31 (MEC 13.3) and EphB4, which were then detected by incubating the sections with fluorescence-labeled secondary antibodies [fluorescein isothiocyanate (FITC)–labeled rabbit anti–rat immunoglobulin; biotinylated rabbit anti–goat immunoglobulin; DAKO] and R-Phycoerythrin (RPE)-labeled streptavidin (DAKO).

For histochemical detection of cell proliferation in tumor tissue, frozen sections were fixed in 4% PFA for 15 minutes, blocked with PBS containing 1% FCS and 0.2% Tween for 30 minutes, and incubated with anti–rabbit phospho-H3 antibody in a humid chamber for 60 minutes. Phospho-H3 was preferred over PCNA or Ki67 as it is detectable in a narrow window of the cell cycle detecting M-phase cells.

Following washes, the secondary antibody (FITC-labeled goat anti–rabbit IgG; Dianova, Hamburg, Germany) was incubated for 30 minutes and counterstained with 4′,6-Diamidine-2′-phenylindole dihydrochloride (DAPI). Apoptosis was assessed using an apoptosis detection kit according to the manufacturer's instructions (Immunotech, Marseille, France). Slides were quantitatively analyzed by counting the number of positive cells in 10 randomly selected microscopic fields of view (high magnification, × 200) of two sections of each tumor.

Statistical Analysis

All results are expressed as mean ± SD unless indicated otherwise. Differences between experimental groups were analyzed by unpaired Student's *t*-test. *P* values < .05 were considered statistically significant.

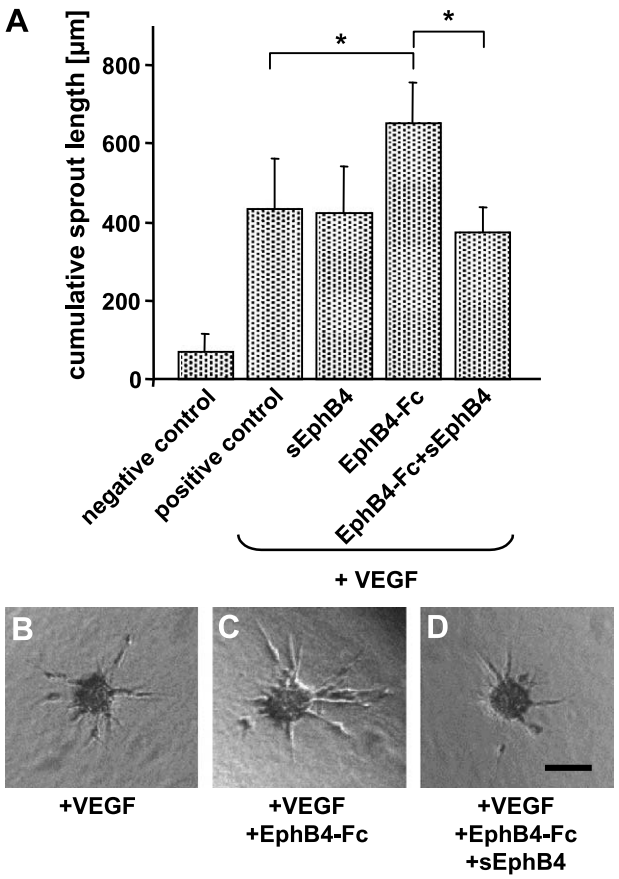

Figure 1. *Effect of monomeric and dimeric soluble EphB4 on gel sprouting angiogenesis. Concentrations as low as 2 ng/ml VEGF induce a robust sprouting angiogenesis effect originating from collagen gel–embedded HUVEC spheroids (negative control versus positive control) (A and B). Dimeric EphB4-Fc (5 µg/ml) significantly enhances VEGF-induced sprouting angiogenesis (*P < .05) (A and C). In contrast, soluble monomeric EphB4 (5 µg/ml) does not affect VEGF-induced sprouting angiogenesis. An excess of monomeric sEphB4 (25 µg/ml), however, completely abrogates EphB4-Fc induced sprouting angiogenesis (*P < .05) (A and D). Scale bar, 100 µm.*

Results

EphB4-Induced Capillary Sprout Formation Is Inhibited by Soluble Monomeric EphB4

HUVECs express ephrinB2, and activation of reverse endothelial ephrinB2 signaling by dimeric or clustered EphB4-Fc stimulates sprouting angiogenesis [13]. We employed a spheroidal three-dimensional *in vitro* angiogenesis assay [32] to study if dimeric EphB4 is also capable of enhancing VEGF-induced proangiogenic effects. Sprouting of HUVECs originating from collagen gel–embedded spheroids can be robustly stimulated with concentrations of VEGF as low as 2 ng/ml (Figure 1, *A* and *B*). Dimeric EphB4-Fc does not just stimulate capillary sprouting on its own, but also enhances VEGF induced in gel sprouting angiogenesis (Figure 1, *A* and *C*). In turn, monomeric soluble EphB4 consisting of the extracellular domain of EphB4 does not affect basal or VEGF-induced sprouting angiogenesis, but completely blocks EphB4-Fc–induced enhancement of VEGF-induced sprouting angiogenesis (Figure 1, *A* and *D*). Despite the lower avidity of monomeric sEphB4 compared to dimeric EphB4-Fc (data not shown), these experiments demonstrate the ability of excess monomeric sEphB4 to functionally neutralize ephrinB2 signaling–mediated proangiogenic effects.

Growth of sEphB4-Expressing A375 Tumors Is Dramatically Impaired

Based on the observed *in vitro* angioinhibitory effects of sEphB4, we generated constitutively sEphB4-expressing A375 melanoma cells in order to study the effect of sEphB4 on tumor growth and angiogenesis. A375 melanoma cells were employed for these experiments in consideration of their robust angiogenic phenotype associated, among others, with intense VEGF, VEGF-C, and Ang-1 expression (Ref. [30] and unpublished data). Likewise, RT-PCR screening experiments had confirmed that A375 cells do not express EphB4 (Figure 2*A*). Yet, further analyses identified A375 cells as an $EphB1^+$, $EphB2^+$, and $ephrinB2^+$ cell population (Figure 2*A*). Transfected A375 cells express abundant amounts of sEphB4 as evidenced by an intense Northern blot signal (Figure 2*B*) as well as the detection of sEphB4 protein in the supernatant of transfected cells (Figure 2*C*). We had opted to employ monomeric sEphB4 in consideration of the fact that dimeric sEphB4-Fc acts agonistically and proangiogenically on reverse EphrinB2 signaling (Figure 1) [13,33] similar to the proangiogenic function of reverse ephrinB1 signaling [34]. Dimeric sEphB4-Fc was found to enhance VEGF-induced angiogenesis *in vivo* in a subcutaneous chamber model, whereas monomeric sEphB4 inhibited VEGF-induced angiogenesis in this model (Martiny-Baron et al., unpublished observations).

Soluble EphB4-expressing and mock-transfected A375 melanoma cells were subcutaneously implanted into nude mice. Mock-transfected A375 cells show an exponential growth curve (Figure 2*D*) corresponding to the growth of the parental cells and grow to a tumor weight of about 1 g (Figure 2, *E* and *F*). In contrast, sEphB4-expressing tumors

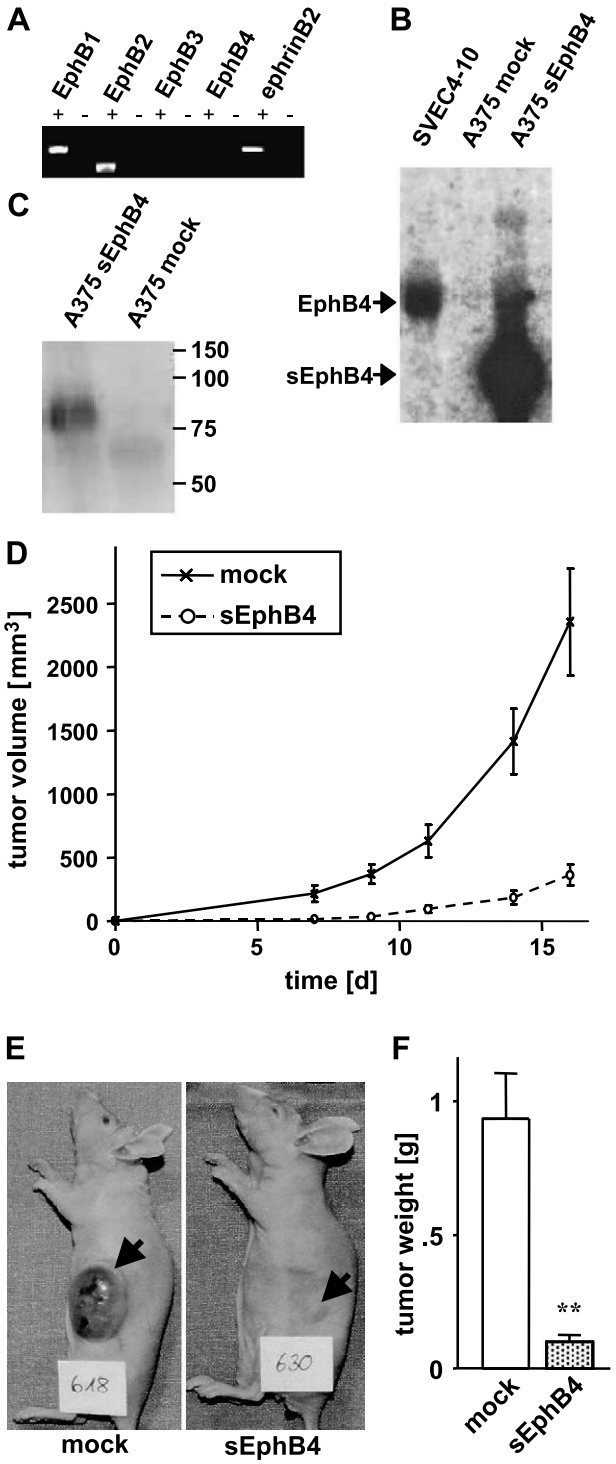

Figure 2. *Growth of sEphB4-expressing and mock-transfected A375 melanomas. Wild-type A375 cells express the receptors EphB1 and EphB2 as well as the EphB2/B3/B4 ligand, ephrinB2. Expression of the receptors EphB3 and EphB4 is not detectable by RT-PCR analysis (A). Constitutively sEphB4-transfected cells abundantly express sEphB4 mRNA (B) (Northern blot) and sEphB4 protein (C) (Western blot analysis of supernatant; SVEC4-10 cells expressing endogenous full-length EphB4 used as control). Subcutaneous injection of A375 cells (106 each) into nude mice leads to rapid tumor growth (D and F). Mock-transfected tumors form reddish tumors indicative of intense vascularization (E). In contrast, sEphB4-expressing A375 melanomas form small subcutaneous nodules (E) with strongly reduced total tumor weight (F) (**P <0.001). The figure shows the mean ± SEM of one of three experiments with similar results analyzing at least 12 mice per data point.*

grow significantly more slowly (Figure 2*D*), which leads to the formation of small tumors with a tumor weight below 0.2 g (Figure 2, *E* and *F*).

Microvessel Density Is Moderately Reduced in sEphB4-Expressing Tumors

Vessel density of sEphB4 and mock-transfected A375 tumors was assessed by counting $CD34^+$ microvessels. A375 melanomas have a prominent proangiogenic phenotype [30] as evidenced by a dense network of microvessels (Figure 3, *A* and *C*). Total microvessel density in sEphB4-expressing tumors is moderately reduced by 19% ($P < .05$; Figure 3, *B* and *C*). Colocalization of the endothelial cell marker, CD31, with the mural cell marker, desmin, identified a subtle, nonsignificant difference of mural cell coverage of tumor microvessels (36.3 ± 7.6% *vs* 28.4 ± 8.0%).

For a more detailed analysis of the phenotype of sEphB4-expressing tumors, we developed an EphB4/CD31 double-staining technique, which revealed marked variations in the intensity of sEphB4 expression in different areas of the tumor. Areas with the highest sEphB4 levels were found to correspond to low microvessel densities (Figure 3, *D* and *E*). Likewise, microvessels in areas with the highest sEphB4 expression had a disturbed morphology when compared to tumor areas with low sEphB4 expression or mock-transfected tumors. Altered vascular morphology was characterized by very small immunoreactive CD31 spots indicative of collapsed vessels without lumen (Figure 3*E*).

Soluble EphB4-Expressing A375 Melanoma Cells Cannot Form Proper Adhesive Contacts and Have Reduced Rates of Proliferation and Apoptosis In Vitro and In Vivo

Soluble EphB4 significantly inhibited tumor angiogenesis (Figure 3). Yet, the moderate inhibition of angiogenesis was not likely to be solely responsible for the dramatic tumor-inhibitory effect of sEphB4 (Figure 2). We therefore hypothesized that the dramatic tumor-inhibitory effect of sEphB4 expression in A375 melanomas may have been the consequence of a combined antiangiogenic and antitumorigenic effect of sEphB4, and have decided to characterize the properties of sEphB4-expressing A375 cells in more detail. Short-term thymidine incorporation experiments did not reveal a difference in the proliferation of sEphB4-transfected cells and mock-transfected cells grown in monolayer culture (data not shown). Likewise, direct counting of proliferating cells showed identical proliferation kinetics for the first 4 days, after which the two cell populations started to diverge (Figure 4*A*). Yet, this difference turned out to be nonsignificant when comparing growth rates (comparison of log-transformed proliferation data). Both sEphB4 and mock-transfected cells were similarly capable of anchorage-independent growth as evidenced by their ability to form colonies in soft agar with comparable growth properties within the first few days. However, sEphB4-transfected A375 cells formed smaller colonies after 14 days in culture (Figure 4, *B* and *C*). We therefore analyzed the cell cycle distribution of mock and sEphB4-transfected A375 cells grown for 13 days in soft agar. Soluble EphB4-transfected cells had significantly

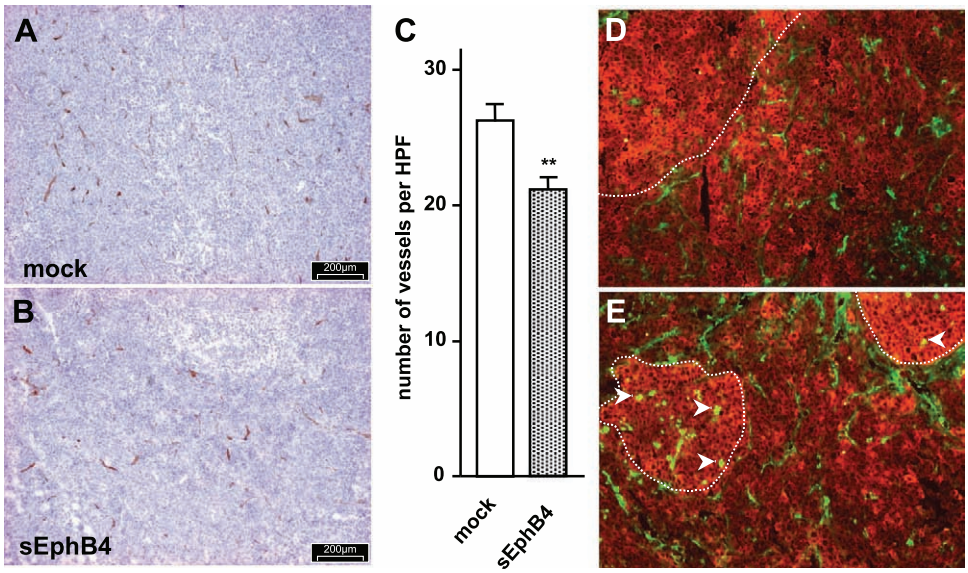

Figure 3. *Vascularization of mock-transfected (A) and sEphB4-expressing (B) A375 melanomas. Tumor sections were stained for the endothelial cell marker, CD34, and the microvessel density was quantitated in at least five high-power fields per tumor section. Total microvessel density is reduced by approximately 20% in sEphB4-expressing tumors (**P < 0.01) (C). The figure shows the mean±SEM of one of three experiments with similar results, analyzing at least 14 tumor sections per experimental group. Double staining for the endothelial cell marker, CD31 (green fluorescence), and for sEphB4 expression (red fluorescence) identified a heterogeneous intratumoral sEphB4 expression pattern with areas of the highest expression (dotted line) being adjacent to areas of lower expression. Regions of high sEphB4 expression correspond to the regions with the lowest microvessel density (D, upper left area). Likewise, microvessels in low sEphB4 areas can regularly be identified as elongated lumenized structures, whereas microvessels in high sEphB4-expressing areas are characterized by small CD31$^+$ dots indicative of collapsed vessels (E, dotted lines).*

reduced numbers of sub-G1 cells (14.5% *vs* 3.5%, $P < .01$) indicating an altered turnover of the cells (Figure 4, *D* and *E*). The most dramatic phenotypic difference between sEphB4 and mock-transfected cells was observed when assessing their intercellular adhesiveness in three-dimensional spheroid assays. Mock-transfected cells formed compacted round spheroidal aggregates. In turn, sEphB4-transfected cells could not form spheroids, but rather organized into a sheet of loosely adherent cells (Figure 4, *F* and *G*).

The observed cell–cell interaction differences (adhesion, spheroidal organization, and size and cell cycle distribution of soft agar colonies) prompted us to further study proliferation and apoptosis in the wild-type and sEphB4-expressing tumors. Staining of the tumor sections for Ki67 identified that the vast majority of the cells were uniformly Ki67$^+$. We therefore employed an anti–phospo-H3 antibody, which identifies M-phase cells and can therefore be used as a proliferation marker that identifies a narrower window of the cell cycle. Phospho-H3 staining detected significantly lower numbers of mitotic tumor cells in the sEphB4-expressing tumors compared to the mock-transfected tumors (Figure 4*H*). Surprisingly and corresponding to the soft agar cell cycle distribution experiments, sEphB4-expressing tumors also had significantly reduced levels of apoptosis as detected by transferase-mediated dUTP nick end labeling (TUNEL) staining (Figure 4 *I*). Collectively, the detailed analysis of sEphB4-transfected A375 cells *in vitro* and *in vivo* showed that tumorigenicity (soft agar assay) and cell proliferation in planar cell culture systems as such are not affected by sEphB4. Yet, sEphB4 acts to interfere with tumor cell–cell communication as evidenced by a perturbed cell adhesion phenotype and, concomitantly, reduced cell proliferation and apoptosis.

Expression of EphB4 Is Enhanced in Colon Cancer

The above analysis of sEphB4-expressing A375 tumors suggested that EphB/ephrinB signaling controls multiple endothelial cell and tumor cell interactions related to tumor progression and that sEphB4 interferes with tumor growth and angiogenesis in EphB/ephrinB2–expressing tumors. EphB4 and ephrinB2 have recently been shown to be expressed by epithelial cells in the intestines, where they control the spatial organization of differentiating epithelial cells toward each other [14]. We therefore analyzed the expression of EphB4 and ephrinB2 in human colon tumors. RNA was isolated from 15 matched pairs of colon tumor tissues and adjacent tumor cell–free tissue biopsies and was analyzed by Northern blot. EphrinB2 was found to be expressed at the same level in tumor and adjacent tissues (Figure 5, *A* and *B*). In contrast, EphB4 expression was found to be two-fold upregulated in colon carcinoma tissues ($P < .001$) (Figure 5, *A* and *B*).

Discussion

A number of different avenues have been developed to therapeutically interfere with tumor angiogenic signaling mechanisms including antibodies to angiogenic cytokines [35] and their receptors [36], dominant-negative receptors [37], and soluble receptors, which have been used widely as cytokine traps to therapeutically interfere with tumor-associated angiogenesis [30,38–40].

EphB receptors and their corresponding ephrinB ligands have been shown to be critically involved in vascular morphogenesis [9]. Yet, they have not been explored much as therapeutic target to interfere with tumor growth and angiogenesis. EphB receptor–expressing cells engage bidirectional signal transduction mechanisms on interaction with corresponding ephrinB ligand–expressing cells. As such, dimeric (or clustered) soluble EphB receptors competitively inhibit EphB receptors. Yet, they may also act as agonists of reverse signaling in ephrinB ligand–expressing cells. Reverse signaling ephrinB2 activation by dimeric (or clustered) soluble EphB4 elicits a proangiogenic effect [13], contributing to the arteriolizing effect of ephrinB2 [9]. We have consequently studied the effect of soluble monomeric EphB4 (sEphB4) on tumor growth and angiogenesis. The experiments show that: 1) sEphB4 inhibits gel sprouting angiogenesis induced by dimeric EphB4-Fc; 2) sEphB4 dramatically inhibits growth of sEphB4-expressing A375 melanomas; 3) sEphB4 interferes with tumor angiogenesis and vessel organization; 4) sEphB4 does not affect primary tumorigenicity parameters of A375 cells, but interferes with tumor cell–cell adhesion and affects cell proliferation and apoptosis in three-dimensional systems *in vitro* and *in vivo*; and 5) EphB4 is upregulated in human colon cancers.

The experiments suggest that the EphB/ephrinB system may offer an attractive molecular system as a therapeutic target. Originally believed to exclusively act by providing positional guidance cues during neuronal patterning, the rate-limiting role of EphB receptors and ephrinB ligands in vascular patterning is now well established [9]. Furthermore, EphB receptors and ephrinB ligands have been shown to control spatial organization of intestinal epithelial cells [14]. Corresponding to these findings, we observed significantly upregulated levels of EphB4 expression in colon cancers, confirming and extending the findings by Liu et al. [16] and Stephenson et al. [23]. We did not observe an overexpression of ephrinB2 in colon cancers, which is prominently expressed by angiogenic endothelial cells [10,11]. This lack of detectable ephrinB2 overexpression in our Northern blot screening experiments of colon carcinomas is most likely

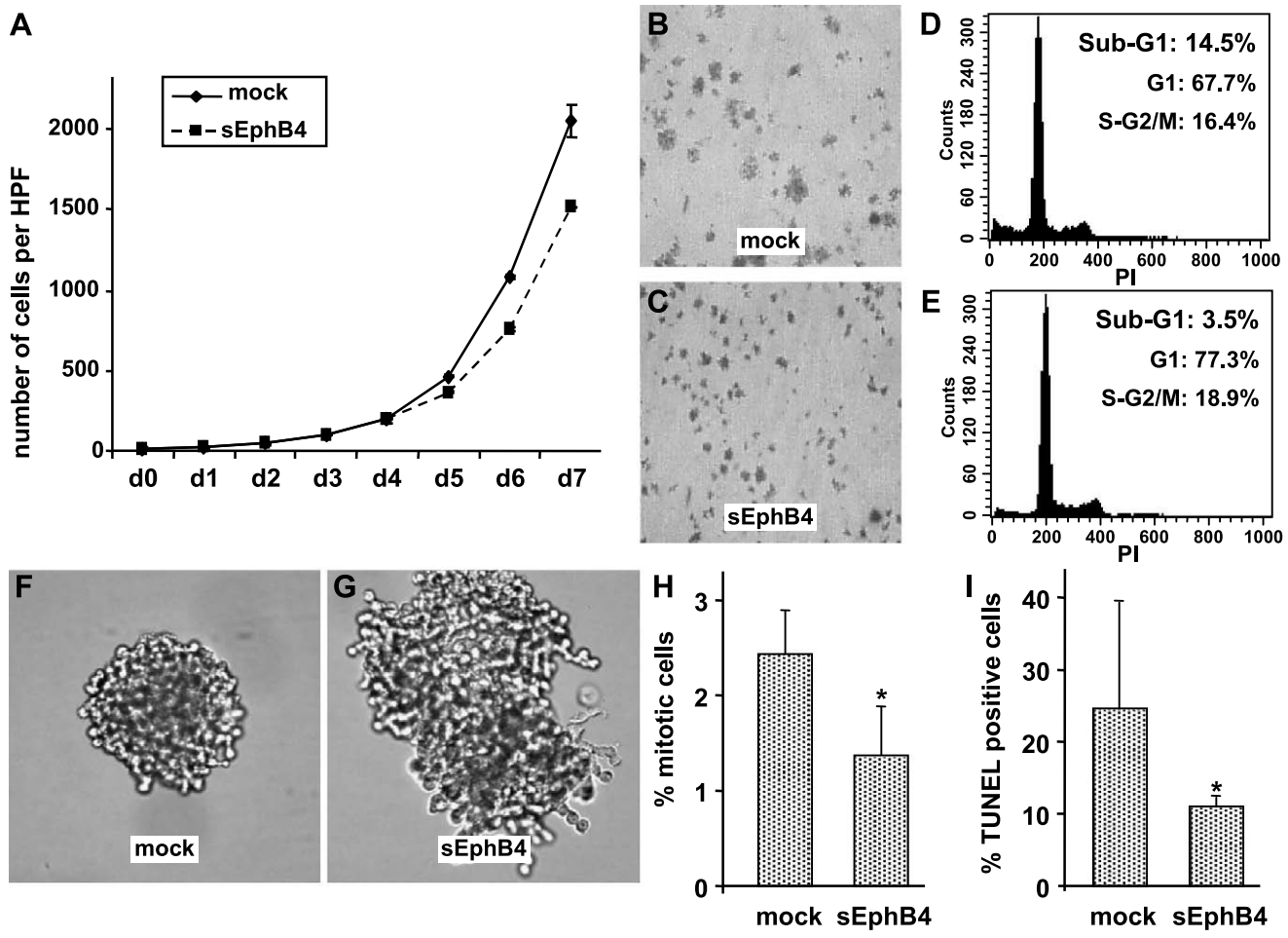

Figure 4. *Analysis of mock-transfected wild-type and sEphB4-expressing A375 melanoma cells in culture and tumors. Expression of sEphB4 has only a minor effect on proliferation of A375 as evidenced by a nonsignificant difference in the tumor cells' growth rate (A) (n = 3 in duplicates). Likewise, both sEphB4-transfected and mock-transfected cells similarly form colonies in a 14-day soft agar assay (B and C). Yet, colonies of sEphB4-expressing cells remain smaller (B versus C) and the cells have an altered cell cycle distribution pattern with significantly reduced levels of sub-G1 cells (n = 3; P < .05) (D and E). Mock-transfected A375 cells form compact three-dimensional spheroids (F). In contrast, sEphB4-expressing A375 cells do not form compacted three-dimensional spheroids (G). Soluble EphB4-expressing A375 tumors contain significantly less mitotic cells as evidenced by staining with an anti–phospho-H3 antibody (H) and fewer TUNEL⁺ cells (I) (n = 4; *P < .05).*

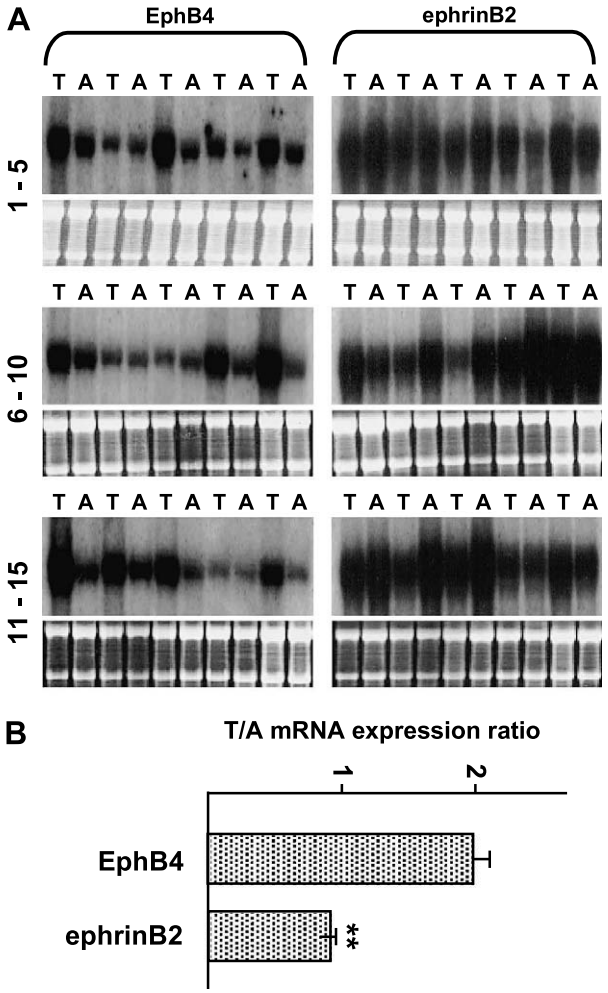

Figure 5. *Expression of EphB4 and ephrinB2 mRNA in matched pairs of colon carcinomas and adjacent normal tissue. (A) Total RNA isolated from biopsies of tumor (T) and adjacent (A) tissues from 15 patients was isolated and analyzed by Northern blot analysis (upper panel; lower panel: 28S and 18S loading controls). (B) Ratio of tumor versus adjacent normal tissue (T/A) expression levels of EphB4 and ephrinB2 quantitated by comparative densitometric analysis of Northern blot signals (normalized to loading controls). Relative ephrinB2 expression levels do not differ in colon tumors and adjacent normal tissue. In contrast, EphB4 expression is two-fold upregulated in human colon cancers (**P < .001).*

reflective of the strong dilution of the endothelial cell–derived Northern blot signal by the vast majority of ephrinB2-expressing tumor cells. In turn, it also highlights the necessity for a strong purification of the endothelial cell compartment in any kind of angiogenesis-related genomic screening effort [41].

The dramatic therapeutic effect of sEphB4 on the growth of A375 melanomas is the result of interfering with multiple EphB/ephrinB2 interactions that govern both tumor cell and angiogenic endothelial cell properties at later stages of tumor progression. Soluble EphB4 reduces intratumoral microvessel density by approximately 20%. This may not be sufficient to account for the observed potent antitumorigenic effect. Instead, direct antitumorigenic effects are also elicited as a consequence of sEphB4 expression. This was surprising as A375 cells do not express EphB4. Yet, they do express EphB2, which is also a receptor for ephrinB2. Consequently, the blocking of ephrinB2 by sEphB4 also interferes with EphB2/ephrinB2 interactions. Soluble EphB4 does not directly affect tumor cell proliferation. Instead, it affects the tumor cells' ability to form proper cell–cell contacts, resulting in the formation of small colonies in soft agar experiments even though soft agar colony formation as such is not affected by sEphB4. Rates of cell proliferation and apoptosis are both reduced *in vivo*. It appears likely that the dominance of reduced proliferation over the reduced rate of apoptosis is likely to account for the observed reduction in tumor growth.

Taken together, the data strongly suggest that the dramatic tumor growth–inhibitory effect in the sEphB4-expressing tumors has resulted from a combined antiangiogenic and antitumorigenic effect. Likewise, multicompartment expression of EphB receptors and ephrinB ligands by endothelial cells and tumor cells may also suggest that EphB/ephrinB signaling may not just control interactions between tumor cells and between endothelial cells, but also drive tumor endothelial cell interactions. As such, it will be interesting to study if Eph/ephrin interactions are capable of controlling tumor cell dissemination mechanisms as they relate to metastasis.

The present study has shown that sEphB4 exerts dual effects by affecting both the tumor and the vascular compartment. It is tempting to speculate on the multiple cellular interactions that are governed by bidirectional EphB/ephrinB signaling during tumor progression and metastasis. What was originally identified as a presumably neuronal-specifically acting molecular system [6] is now emerging as a universal cell–cell interaction and communication regulating system that transduces positional information to the cells of the vascular system [7–9], the intestinal system [14], different tumor types [15–17], and likely other hitherto not yet identified cells and organs. Given the multicompartment and multicellular character of the EphB/ephrinB system, it is likely that additional EphB/ephrinB–regulated cell–cell interactions will be uncovered in the near future. It also suggests that the EphB/ephrinB system may emerge as an attractive therapeutic target for a number of pathological conditions.

Monomeric sEphB4 interferes potently with growth and angiogenesis of A375 melanomas. Yet, these findings need to be interpreted as proof-of-principle experiments aimed at exploring the EphB/ephrinB axis as a potential antitumorigenic therapeutic target. Monomeric receptors are notoriously known as poor inhibitors due to their low affinity and avidity compared to dimeric or clustered receptors [38]. This was reflected in the present study by the requirement to employ excess amounts of monomeric sEphB4 to inhibit dimeric EphB4-Fc induced in gel sprouting angiogenesis (Figure 1). We observed that the antivascular effect of sEphB4 was most pronounced in intratumoral areas with highest sEphB4 expression (Figure 3). Recent experiments have proposed a scheme to design multidomain high-affinity receptor bodies as antagonizing cytokine traps, which will also allow an attractive avenue toward the development of reagents that can therapeutically interfere with Eph/ephrin signaling [38].

Taken together, the present study has shown that EphB/ephrinB interactions are critically involved in tumor progression and angiogenesis and offer an attractive therapeutic

target that is also supported by the growing list of human tumors that overexpress EphB receptors or ephrinB ligands, including colon cancers (this study and Refs. [16,23]), melanomas [24], endometrial tumors [25], neuroblastomas [27,28], and gastric tumors [42]. The experiments offer an attractive rationale for the development of specific high-affinity biological and small-molecular-weight pharmacological inhibitors of Eph/ephrin signaling. They also highlight the complexity of Eph/ephrin–driven cellular interactions controlling the tumor cell as well as the vascular compartment. Future work aimed at studying the complexity of the multicompartment Eph/ephrin signaling network may well shed further light into the complexity of tumor cell–endothelial cell interactions and contribute to a better understanding of tumor progression mechanisms as they relate to metastatic dissemination of tumor cells.

Acknowledgements

The authors thank Stefanie Koidl and Kerstin Leptien for excellent technical assistance, and Ralph Graeser for help with the phospho-H3 immunohistochemistry.

References

[1] Klein R (2001). Excitatory Eph receptors and adhesive ephrin ligands. *Curr Opin Cell Biol* **13,** 196–203.

[2] Kullander K and Klein R (2002). Mechanisms and functions of Eph and ephrin signalling. *Nat Rev Mol Cell Biol* **3,** 475–486.

[3] Schmucker D and Zipursky SL (2001). Signaling downstream of Eph receptors and ephrin ligands. *Cell* **105,** 701–704.

[4] Bruckner K, Pasquale EB, and Klein R (1997). Tyrosine phosphorylation of transmembrane ligands for Eph receptors. *Science* **275,** 1640–1643.

[5] Holland SJ, Gale NW, Mbamalu G, Yancopoulos GD, Henkemeyer M, and Pawson T (1996). Bidirectional signalling through the EPH-family receptor Nuk and its transmembrane ligands. *Nature* **383,** 722–725.

[6] Orioli D and Klein R (1997). The Eph receptor family: axonal guidance by contact repulsion. *Trends Genet* **13,** 354–359.

[7] Wang HU, Chen ZF, and Anderson DJ (1998). Molecular distinction and angiogenic interaction between embryonic arteries and veins revealed by ephrin-B2 and its receptor Eph-B4. *Cell* **93,** 741–753.

[8] Adams RH, Wilkinson GA, Weiss C, Diella F, Gale NW, Deutsch U, Risau W, and Klein R (1999). Roles of ephrinB ligands and EphB receptors in cardiovascular development: demarcation of arterial/venous domains, vascular morphogenesis, and sprouting angiogenesis. *Genes Dev* **13,** 295–306.

[9] Adams RH (2002). Vascular patterning by Eph receptor tyrosine kinases and ephrins. *Semin Cell Dev Biol* **13,** 55–60.

[10] Gale NW, Baluk P, Pan L, Kwan M, Holash J, DeChiara TM, McDonald DM, and Yancopoulos GD (2001). Ephrin-B2 selectively marks arterial vessels and neovascularization sites in the adult, with expression in both endothelial and smooth muscle cells. *Dev Biol* **230,** 151–160.

[11] Shin D, Garcia-Cardena G, Hayashi SI, Gerety S, Asahara T, Stavrakis G, Isner J, Folkman J, Gimbrone MA, and Anderson DJ (2001). Expression of ephrinB2 identifies a stable genetic difference between arterial and venous vascular smooth muscle as well as endothelial cells, and marks subsets of microvessels at sites of adult neovascularization. *Dev Biol* **230,** 139–150.

[12] Adams RH, Diella F, Hennig S, Helmbacher F, Deutsch U, and Klein R (2001). The cytoplasmic domain of the ligand ephrinB2 is required for vascular morphogenesis but not cranial neural crest migration. *Cell* **104,** 57–69.

[13] Füller T, Korff T, Kilian A, Dandekar G, and Augustin HG (2003). Forward EphB4 signaling in endothelial cells controls cellular repulsion and segregation from ephrinB2 positive cells. *J Cell Sci* **116,** 2461–2470.

[14] Batlle E, Henderson JT, Beghtel H, van den Born MM, Sancho E, Huls G, Meeldijk J, Robertson J, van de Wetering M, Pawson T, and Clevers H (2002). Beta-catenin and TCF mediate cell positioning in the intestinal epithelium by controlling the expression of EphB/ephrinB. *Cell* **111,** 251–263.

[15] Dodelet VC and Pasquale EB (2000). Eph receptors and ephrin ligands: embryogenesis to tumorigenesis. *Oncogene* **19,** 5614–5619.

[16] Liu W, Ahmad SA, Jung YD, Reinmuth N, Fan F, Bucana CD, and Ellis LM (2002). Coexpression of ephrin-Bs and their receptors in colon carcinoma. *Cancer* **94,** 934–939.

[17] Ogawa K, Pasqualini R, Lindberg RA, Kain R, Freeman AL, and Pasquale EB (2000). The ephrin-A1 ligand and its receptor, EphA2, are expressed during tumor neovascularization. *Oncogene* **19,** 6043–6052.

[18] Zelinski DP, Zantek ND, Stewart JC, Irizarry AR, and Kinch MS (2001). EphA2 overexpression causes tumorigenesis of mammary epithelial cells. *Cancer Res* **61,** 2301–2306.

[19] Brantley DM, Cheng N, Thompson EJ, Lin Q, Brekken RA, Thorpe PE, Muraoka RS, Cerretti DP, Pozzi A, Jackson D, Lin C, and Chen J (2002). Soluble Eph A receptors inhibit tumor angiogenesis and progression *in vivo*. *Oncogene* **21,** 7011–7026.

[20] Carles-Kinch K, Kilpatrick KE, Stewart JC, and Kinch MS (2002). Antibody targeting of the EphA2 tyrosine kinase inhibits malignant cell behavior. *Cancer Res* **62,** 2840–2847.

[21] Nakamoto M and Bergemann AD (2002). Diverse roles for the Eph family of receptor tyrosine kinases in carcinogenesis. *Microsc Res Tech* **59,** 58–67.

[22] Chen E, Xia G, Kundra A, Smith DL, Masood R, and Gill P (2003). EphB4/ephrinB2 expression by malignant mesothelioma as a potential therapeutic target. *Proc Am Assoc Cancer Res* **44,** 475.

[23] Stephenson SA, Slomka S, Douglas EL, Hewett PJ, and Hardingham JE (2001). Receptor protein tyrosine kinase EphB4 is up-regulated in colon cancer. *BMC Mol Biol* **2,** 15.

[24] Vogt T, Stolz W, Welsh J, Jung B, Kerbel RS, Kobayashi H, Landthaler M, and McClelland M (1998). Overexpression of Lerk-5/Eplg5 messenger RNA: a novel marker for increased tumorigenicity and metastatic potential in human malignant melanomas. *Clin Cancer Res* **4,** 791–797.

[25] Takai N, Miyazaki T, Fujisawa K, Nasu K, and Miyakawa I (2001). Expression of receptor tyrosine kinase EphB4 and its ligand ephrin-B2 is associated with malignant potential in endometrial cancer. *Oncol Rep* **8,** 567–573.

[26] Nikolova Z, Djonov V, Zuercher G, Andres AC, and Ziemiecki A (1998). Cell-type specific and estrogen dependent expression of the receptor tyrosine kinase EphB4 and its ligand ephrinB2 during mammary gland morphogenesis. *J Cell Sci* **111,** 2741–2751.

[27] Tang XX, Evans AE, Zhao H, Cnaan A, London W, Cohn SL, Brodeur GM, and Ikegaki N (1999). High-level expression of EPHB6, EFNB2, and EFNB3 is associated with low tumor stage and high TrkA expression in human neuroblastomas. *Clin Cancer Res* **5,** 1491–1496.

[28] Tang XX, Zhao H, Robinson ME, Cohen B, Cnaan A, London W, Cohn SL, Cheung NK, Brodeur GM, Evans AE, and Ikegaki N (2000). Implications of EPHB6, EFNB2, and EFNB3 expressions in human neuroblastoma. *Proc Natl Acad Sci USA* **97,** 10936–10941.

[29] Drevs J, Müller-Driver R, Wittig C, Fuxius S, Esser N, Hugenschmidt H, Konerding MA, Allegrini PR, Wood J, Hennig J, Unger C, and Marme D (2002). PTK787/ZK 222584, a specific vascular endothelial growth factor-receptor tyrosine kinase inhibitor, affects the anatomy of the tumor vascular bed and the functional vascular properties as detected by dynamic enhanced magnetic resonance imaging. *Cancer Res* **62,** 4015–4022.

[30] Siemeister G, Schirner M, Weindel K, Reusch P, Menrad A, Marme D, and Martiny-Baron G (1999). Two independent mechanisms essential for tumor angiogenesis: inhibition of human melanoma xenograft growth by interfering with either the vascular endothelial growth factor receptor pathway or the Tie-2 pathway. *Cancer Res* **59,** 3185–3191.

[31] Korff T and Augustin HG (1998). Integration of endothelial cells in multicellular spheroids prevents apoptosis and induces differentiation. *J Cell Biol* **143,** 1341–1352.

[32] Korff T and Augustin HG (1999). Tensional forces in fibrillar extracellular matrices control directional capillary sprouting. *J Cell Sci* **112,** 3249–3258.

[33] Hamada K, Oike Y, Ito Y, Maekawa H, Miyata K, Shimomura T, and Suda T (2003). Distinct roles of ephrin-B2 forward and EphB4 reverse signaling in endothelial cells. *Arterioscler Thromb Vasc Biol* **23,** 190–197.

[34] Huynh-Do U, Vindis C, Liu H, Cerretti DP, McGrew JT, Enriquez M, Chen J, and Daniel TO (2002). Ephrin-B1 transduces signals to activate integrin-mediated migration, attachment and angiogenesis. *J Cell Sci* **115,** 3073–3081.

[35] Ferrara N (2002). Role of vascular endothelial growth factor in physiologic and pathologic angiogenesis: therapeutic implications. *Semin Oncol* **29,** 10–14.

[36] Witte L, Hicklin DJ, Zhu Z, Pytowski B, Kotanides H, Rockwell P, and Bohlen P (1998). Monoclonal antibodies targeting the VEGF receptor-2 (Flk1/KDR) as an anti–angiogenic therapeutic strategy. *Cancer Metastasis Rev* **17,** 155–161.

[37] Millauer B, Longhi MP, Plate KH, Shawver LK, Risau W, Ullrich A, and Strawn LM (1996). Dominant-negative inhibition of Flk-1 suppresses the growth of many tumor types *in vivo*. *Cancer Res* **56,** 1615–1620.

[38] Economides AN, Carpenter LR, Rudge JS, Wong V, Koehler-Stec EM, Hartnett C, Pyles EA, Xu X, Daly TJ, Young MR, Fandl JP, Lee F, Carver S, McNay J, Bailey K, Ramakanth S, Hutabarat R, Huang TT, Radziejewski C, Yancopoulos GD, and Stahl N (2003). Cytokine traps: multi-component, high-affinity blockers of cytokine action. *Nat Med* **9,** 47–52.

[39] Holash J, Davis S, Papadopoulos N, Croll SD, Ho L, Russell M, Boland P, Leidich R, Hylton D, Burova E, Ioffe E, Huang T, Radziejewski C, Bailey K, Fandl JP, Daly T, Wiegand SJ, Yancopoulos GD, and Rudge JS (2002). VEGF-Trap: a VEGF blocker with potent antitumor effects. *Proc Natl Acad Sci USA* **99,** 11393–11398.

[40] Barleon B, Siemeister G, Martiny-Baron G, Weindel K, Herzog C, and Marme D (1997). Vascular endothelial growth factor up-regulates its receptor fms-like tyrosine kinase 1 (FLT-1) and a soluble variant of FLT-1 in human vascular endothelial cells. *Cancer Res* **57,** 5421–5425.

[41] St Croix B, Rago C, Velculescu V, Traverso G, Romans KE, Montgomery E, Lal A, Riggins GJ, Lengauer C, Vogelstein B, and Kinzler KW (2000). Genes expressed in human tumor endothelium. *Science* **289,** 1197–1202.

[42] Kataoka H, Tanaka M, Kanamori M, Yoshii S, Ihara M, Wang YJ, Song JP, Li ZY, Arai H, Otsuki Y, Kobayashi T, Konno H, Hanai H, and Sugimura H (2002). Expression profile of EFNB1, EFNB2, two ligands of EPHB2 in human gastric cancer. *J Cancer Res Clin Oncol* **128,** 343–348.